

doi: 10.1093/cercor/bhab100 Original Article

ORIGINAL ARTICLE

Functional Realignment of Frontoparietal Subnetworks during Divergent Creative Thinking

Roger E. Beaty¹, Robert A. Cortes², Daniel C. Zeitlen¹, Adam B. Weinberger^{2,3} and Adam E. Green²

¹Department of Psychology, Pennsylvania State University, University Park, PA 16801, USA, ²Department of Psychology, Georgetown University, Washington, DC 20057, USA and ³Center for Neuroaesthetics, University of Pennsylvania, Philadelphia, PA 19104, USA

Address correspondence to Roger Beaty, Department of Psychology, 140 Moore Building, University Park, PA 16801, USA. Email: rebeaty@psu.edu.

Abstract

Creative cognition has been consistently associated with functional connectivity between frontoparietal control and default networks. However, recent research identified distinct connectivity dynamics for subnetworks within the larger frontoparietal system—one subnetwork (FPCNa) shows positive coupling with the default network and another subnetwork (FPCNb) shows negative default coupling—raising questions about how these networks interact during creative cognition. Here we examine frontoparietal subnetwork functional connectivity in a large sample of participants (n = 171) who completed a divergent creative thinking task and a resting-state scan during fMRI. We replicated recent findings on functional connectivity of frontoparietal subnetworks at rest: FPCNa positively correlated with the default network and FPCNb negatively correlated with the default network. Critically, we found that divergent thinking evoked functional connectivity between both frontoparietal subnetworks and the default network, but in different ways. Using community detection, we found that FPCNa regions showed greater coassignment to a default network community. However, FPCNb showed overall stronger functional connectivity with the default network—reflecting a reversal of negative connectivity at rest—and the strength of FPCNb-default network connectivity correlated with individual creative ability. These findings provide novel evidence of a behavioral benefit to the cooperation of typically anticorrelated brain networks.

Key words: creativity, default network, divergent thinking, frontoparietal control network, functional connectivity

Neuroscientific investigations of creativity are increasingly focused on the contributions of large-scale cortical networks to creative cognition. Across a range of creative tasks and domains, 2 large-scale networks have emerged as central to creative performance: the frontoparietal (or executive) control network and the default (or default mode) network (Ellamil et al. 2012; Jung et al. 2013; Beaty et al. 2016, 2018, 2019). Frontoparietal and default network (DN) interaction during creative cognition is thought to reflect a coordination of controlled and spontaneous cognitive processes, respectively (Beaty et al. 2016). This cooperative connectivity pattern is notable, however, because the frontoparietal and DNs have previously been shown to work in opposition (Fox et al. 2005; Anticevic et al. 2012). Yet recent evidence points to heterogeneity within the frontoparietal

network, with one subnetwork showing "negative" intrinsic (resting) and task-related connectivity with the DN and another subnetwork showing "positive" connectivity with the DN (Dixon et al. 2018; Murphy et al. 2020). These findings raise questions about whether creative thinking involves a reorganization of functional brain networks, or whether the cooperative functional connectivity observed during creativity is embedded within normative network dynamics. In the present research, we aim to address this question by examining functional connectivity of frontoparietal subnetworks during creative task performance in a large sample of participants (n=171). We also test whether between-subject variation in frontoparietal network dynamics is associated with individual differences in creative thinking ability.

Creative Cognition and Frontoparietal-DN Dynamics

Creativity is a complex construct that involves variegated cognitive, motivational, and contextual elements (Amabile 1983; Finke et al. 1992). Cognitive research on creativity has tended to focus on divergent thinking, or the ability to combine information in new ways to solve open-ended problems. Divergent thinking is thought to require a coordination of associative and executive control processes in the service of generating ideas that are both novel and appropriate. The associative theory of creativity (Mednick 1962) posits that creative thinking involves spreading activation of concepts within semantic memory networks. On this view, coming up with a creative idea requires connecting remote concepts within semantic networks, bypassing common and unoriginal concepts along the way (Kenett and Faust 2019). Executive theories of creativity (Benedek et al. 2014b; Benedek and Fink 2019), in contrast, emphasize the contribution of strategic and controlled aspects of cognition required to manage and direct the creative thought process-inhibiting common associations, strategically searching and selecting information, and maintaining higher order goals (Beaty and Silvia 2012; Benedek et al. 2014b; Green 2016; Volle 2018; Chrysikou 2019; Dygert and Jarosz 2020).

Associative and executive cognitive processes appear to be supported by 2 major brain networks: the DN and the frontoparietal control network (FPCN), respectively (Bendetowicz et al. 2018). The DN is composed of medial frontal, medial temporal, cingulate, precuneus, and inferior parietal cortical regions (Raichle et al. 2001; Raichle 2015). DN activity and connectivity are generally elevated during rest, in comparison to cognitive task engagement, suggesting this network reflects the "default mode" of activation in the brain. Yet much research has demonstrated that the DN is not merely a task-negative network (Spreng 2012): it activates during tasks involving self-referential and internally directed cognitive processes, including episodic memory, social and emotional cognition, mental stimulation, and mind wandering (Buckner et al. 2008; Andrews-Hanna 2012; Andrews-Hanna et al. 2014). The FPCN—also known as the executive control network—is composed of lateral prefrontal and anterior inferior parietal regions (Seeley et al. 2007). FPCN activity and connectivity are broadly associated with cognitive processes requiring the strategic and top-down control of attention and cognition, including working memory, decisionmaking, task-set switching, and response inhibition (Niendam et al. 2012).

Recent network neuroscience research has found that creative cognition involves functional connectivity between FPCN and DN (for reviews, see Beaty et al. 2016, 2019). This connectivity pattern has been reported across studies of both domain-general creative thinking (e.g., divergent thinking) and domain-specific creative performance (e.g., artistic drawing; Ellamil et al. 2012), suggesting that it is a reliable neural correlate of creative performance. In a study of divergent thinking—a cognitive processes requiring idea generation, such as thinking of novel object uses—Beaty et al. (2015) found that the posterior cingulate cortex (PCC) of the DN showed increased functional connectivity with dorsolateral prefrontal cortex of the FPCN. More recently, Beaty et al. (2018) replicated and extended this finding in a larger sample, finding that the strength of functional connectivity between the FPCN and the DN (among other regions) could reliably predict an individual's creative ability. Several other studies on creative cognition

and artistic performance have reported similar interactions between FPCN and DN regions, including studies on divergent thinking (Shi et al. 2018; Adnan et al. 2019a, 2019b; Sunavsky and Poppenk 2020), novel word association (Green et al. 2015; Beaty et al. 2017a), metaphor production (Beaty et al. 2017b), music improvisation (Pinho et al. 2016; Belden et al. 2020), poetry composition (Liu et al. 2015), and artistic drawing (Ellamil et al. 2012). The interaction of FPCN and DN during creative cognition is hypothesized to represent goal-directed, selfgenerated thought, with the DN supporting the generation of ideas and the FPCN supporting the evaluation of those ideas by modifying DN output to meet creative task goals (Beaty et al. 2016). Although FPCN-DN cooperation is consistent in creativity neuroscience, a large neuroscience literature supports their antagonistic relationship: DN regions tend to deactivate when FPCN regions activate, both at rest and during performance on many cognitively demanding tasks.

The role of executive control and the FPCN in creative cognition is consistent with recent work on the neurocognitive underpinnings of creativity and intelligence (Benedek 2018; Jung and Chohan 2019; Frith et al. 2021). According to Jung and Chohan (2019), intelligence and creativity can be conceived along 2 major axes-exploratory behavior and restrained action—corresponding to DN and FPCN, respectively. Recently, Frith et al. (2021) reported a substantial cognitive and neural overlap between general intelligence and divergent thinking. Using machine learning (connectome-based predictive modeling), the authors found nearly half of the brain features (i.e., functional connections) that predicted intelligence also predicted divergent thinking, with a majority of the overlapping features within the FPCN and ventral attention/salience network. Intelligence and creative cognition may thus similarly rely on brain regions and networks that support executive

Frontoparietal Network Fractionation and Relationships to the DN

Foundational work by Fox et al. (2005) demonstrated an antagonistic relationship between a "task-positive network" (comprised of FPCN and dorsal attention network [DAN] regions) and a "task-negative network" (comprised of the DN): activity within task-positive regions (e.g., intraparietal sulcus) correlated positively with other task-positive regions (e.g., dorsolateral prefrontal cortex) but correlated negatively with DN regions (e.g., PCC). In the context of cognitively demanding tasks, DN deactivation is posited to reflect the suppression of task-unrelated thoughts (i.e., mind wandering) to facilitate goal-directed performance. Critically, however, the DN has since been revealed as far more than a passive, task-negative system (Spreng 2012), with DN showing activation during internally directed and selfreferential cognitive processes, such as autobiographical memory retrieval, future simulation, and social cognition, among others (Andrews-Hanna et al. 2014).

Although FPCN and DN show an antagonistic relationship across many tasks, the 2 networks are not always anticorrelated. For instance, both the FPCN and DN are recruited during cognitive tasks that require both goal-directed and selfreferential cognition, such as autobiographical future planning (Spreng et al. 2010). Spreng et al. (2010) found that, compared to a task requiring visuospatial planning (i.e., Tower of Hanoi) which engaged FPCN and the DAN—planning a sequence of autobiographical future events engaged FPCN and DN regions, presumably reflecting the goal-directed manipulation of episodic representations. Even in the most seemingly unconstrained context of mind wandering, a review of neuroimaging studies found consistent activation of both the FPCN and DN (Fox et al. 2015), supporting the notion that mind wandering can be strategically constrained by goal-directed signals from the FPCN. Across all of these cognitive processes, it is presumed that the DN plays a role in generating thoughts via episodic or semantic memory (e.g., future events to plan, ideas that could be creative), while the FPCN strategically evaluates and filters these thoughts according to the task at hand.

Recent work has attempted to clarify how and when FPCN and DN regions cooperate by examining distinct subsystems within the FPCN. Using hierarchical clustering and machine learning classification of functional connectivity patterns within the FPCN, Dixon et al. (2018) identified 2 functionally distinct subnetworks previously characterized in a 17-network parcellation (Yeo et al. 2011): FPCNa and FPCNb. FPCNa consisted of rostrolateral prefrontal cortex, middle and superior frontal gyri, middle temporal gyrus, anterior intraparietal sulcus, and presupplementary motor area; FPCNb consisted of inferior frontal sulcus, posterior superior frontal gyrus, posterior middle temporal gyrus, and intraparietal sulcus. Critically, Dixon et al. found that FPCNa showed stronger functional connectivity with the DN core (medial prefrontal cortex, PCC, angular gyri, and anterior middle temporal gyrus) and that FPCNa-DN connectivity was stronger than FPCNa-DAN connectivity. In contrast, FPCNb showed stronger connectivity with the DAN than the DN. This connectivity pattern was observed in nine different conditions (resting-state and 8 different tasks) across 4 independent samples, highlighting the robustness of the relationships between frontoparietal subnetworks and the DN.

The findings of Dixon et al. were recently extended by a multimodal connectivity analysis of working memory (Murphy et al. 2020). Combining functional and structural connectivity (i.e., diffusion tensor imaging), Murphy et al. (2020) found that the strength of FPCN-DN coupling could be altered by tuning the amplitudes of FPCN subnetworks, indicating that the FPCN governs the functional relationship between FPCN and DN. Moreover, the authors noted that FPCNb is critical to working memory performance, whereas FPCNa is more central to introspective cognition—consistent with prior work (Dixon et al. 2018)—and that working memory performance can be further explained by network competition driven by activation of FPCNb (which is negatively correlated with the DN). Taken together, this recently identified heterogeneity within the FPCN, and its corresponding functional relationships to the DN, substantially enriches the initial characterization of these networks. However, questions remain regarding how these networks interact to support other modes of high-level cognition, such as creative cognition.

The Present Research

Creative cognition has been shown to involve positive functional connectivity between FPCN and DN. Yet recent research has identified heterogeneity within FPCN architecture and corresponding functional relationships to the DN, with one FPCN subnetwork (FPCNa) exhibiting a positive association with the DN and another FPCN subnetwork (FPCNb) exhibiting a negative association with the DN (Dixon et al. 2018). These findings raise the question of how FPCN subnetworks operate during creative cognition: Does functional connectivity of FPCN and DN reflect tonically cooperative interaction dynamics of these

networks (FPCNa-DN), or does such coupling reflect a reversal of otherwise competitive network interactions (FPCNb-DN)? The present research examines this question using a combination of functional connectivity and community network detection techniques applied to resting-state and task-fMRI data from a large neuroimaging sample (n = 171). First, we sought to replicate the resting-state connectivity profiles of the 2 FPCN networks reported in prior work (Dixon et al. 2018; Murphy et al. 2020). Next, we tested the main question of interest by assessing differential connectivity of FPCN subnetworks during divergent creative thinking. To further characterize network relationships associated with divergent thinking, we used a data-driven community detection approach to assess how frontoparietal and DN regions cluster together when participants think creatively. Finally, we addressed 2 questions regarding individual differences: (1) Does baseline connectivity of frontoparietal networks "at rest" predict task-related connectivity? and (2) Does taskrelated connectivity relate to behavioral performance on the creative thinking task?

Given recent work on FPCN subnetwork connectivity (Dixon et al. 2018; Murphy et al. 2020), we hypothesized that, during rest, FPCNa would correlate positively with the DN and FPCNb would correlate negatively with the DN. Critically, during divergent thinking, we hypothesized that both FPCN subnetworks would correlate with the DN, in light of prior findings implicating the larger FPCN and DN in creative cognition. Regarding individual differences, we hypothesized that FPCN connectivity strength at rest would correlate with FPCN connectivity strength during the task, and that FPCN connectivity strength would correlate positively with behavioral performance, though given lack of precedent, we did not have specific hypotheses regarding which subnetwork would show a stronger correlation with behavior.

Method

Participants

Neuroimaging and behavioral data were collected as part of a larger project on the psychology and neuroscience of creativity (see Beaty et al. 2018). The full sample of participants consisted of 186 adults from the University of North Carolina at Greensboro (UNCG) and the surrounding community (129 women, mean age = 22.74 years, standard deviation [SD] = 6.37). Participants completed written consent forms and received up to \$100 for their participation in the multiphase study (magnetic resonance imaging [MRI], cognitive assessment, and dailylife experience sampling). They were right-handed, with normal or corrected-to-normal vision, and reported no history of cognitive impairment, neurological issues, or drugs affecting the central nervous system. Participants were excluded for the following reasons: excessive head movement (mean framewise displacement [FD] > 0.5 mm, n = 4; Power et al. 2012), incomplete behavioral data (i.e., verbal responses to creativity tasks), and software/hardware issues. After exclusions, the final sample consisted of 171 adults (119 females, mean age = 22.73 years, SD = 6.22); 165 participants in the final task sample also completed a resting-state scan. The study procedure was approved by the UNCG Institutional Review Board.

fMRI Task Procedures and Divergent Thinking Assessment

Participants completed 2 tasks during functional imaging in an event-related design: (1) the Alternate Uses Task (AUT) and (2) the Object Characteristics Task (OCT; see Beaty et al. 2015, 2018). The AUT is a widely used assessment of divergent thinking (Guilford 1967; Kaufman et al. 2008). Participants were presented with a series of 23 objects and asked to think of a single creative use for each one; they were encouraged to "think creatively" (Green et al. 2015) and to try to come up with the most original idea they could during the thinking period. The OCT is a common semantic control task in fMRI studies of divergent thinking (Fink et al. 2009; Beaty et al. 2015; Vartanian et al. 2018), and it requires participants to think of the defining physical features of a series of objects (23 trials).

The trial structure consisted of: (1) a jittered fixation cross (4-6 s), (2), a condition cue (3 s), (3) a silent response generation phase (12 s), and (4) a response production phase, during which participants spoke their response into an MRI-compatible microphone (5 s; cf., Benedek et al. 2014a, 2018; Beaty et al. 2017a, 2017b, 2018). Before the fMRI scanning session, participants received thorough instructions and completed several practice trials of both tasks. Following the fMRI task, participants completed a 5-minute resting scan, during which they were asked to relax with their eyes closed.

Verbal responses were transcribed by an experimenter for subsequent assessment of creative quality. In the present study, creative quality was assessed via semantic distance—an objective method that is increasingly used in creativity research to automate creativity assessment using computational semantic models (Green 2016; Kenett 2019; Beaty and Johnson 2020). Semantic distance has shown consistent validity for assessment of divergent creativity—the extent to which ideas/concepts diverge in a semantic space—including high correlations with human creativity ratings (Beaty and Johnson 2020; Dumas et al. 2020) and moderate correlations with other creativity measures (e.g., creative achievement in the arts and sciences; Prabhakaran et al. 2014; Beaty and Johnson 2020). At the neural level, recent work has found that semantic distance and human creativity ratings overlap in terms of functional connectivity patterns at rest (Orwig et al. 2021). Given this finding and prior work reporting correlations between human creativity ratings and functional connectivity between the default and control networks (Beaty et al. 2018), we hypothesized that semantic distance would similarly correlate with default-control connectivity strength. However, given the lack of precedent, we did not have a strong prediction regarding whether semantic distance would correlate with either FPCNa or FPCNb.

Consistent with past work, we computed the semantic similarity between the AUT object words (e.g., brick) and participants' verbal responses, then took the inverse of these values to obtain a measure of distance (Green 2016). To compute semantic distance, we used the online platform, SemDis (semdis.wlu.psu.edu; Beaty and Johnson 2020). The SemDis platform leverages 5 semantic models previously shown to have a strong correspondence with human relatedness judgments (Mandera et al. 2017), including 2 count models (which count the co-occurrences of words in large text corpora) and 3 predict models (which use neural networks to predict a given word from surrounding context words; see Mandera et al. 2017). A benefit of this multimodel approach is that it can mitigate biases introduced by relying on a single model and text corpus, thereby increasing generalizability and reliability (Kenett 2019). Following our prior work (Beaty and Johnson 2020), verbal responses were preprocessed by spell checking and removal of the AUT cue word (and its plurals; e.g., "box" and "boxes"). The preprocessed response

file was then uploaded to the SemDis platform, using the following options: cleaning type = remove filler and clean (removes stop words; e.g., an, a, the), semantic space = all; compositional model = multiplicative. For subsequent fMRI analysis, we used the semdis_factor score, a latent variable comprised of the 5 semantic distance values (Beaty and Johnson 2020).

MRI Data Acquisition and Preprocessing

The MRI protocol and preprocessing pipeline were identical to our prior work (Frith et al. 2021), with the exception of brain network modeling (see Functional Network Construction and Preprocessing).

Participants completed the tasks in a single fMRI run. Wholebrain imaging was performed on a 3 T Siemens Magnetom MRI system (Siemens Medical Systems) using a 16-channel head coil. BOLD-sensitive T2*-weighted functional images were acquired using a single shot gradient-echo echo-planar imaging (EPI) pulse sequence [repetition time (TR) = 2000 ms, echo time (TE) = 30 ms, flip angle = 78° , 32 axial slices, $3.5 \times 3.5 \times 4.0$ mm, distance factor 0%, field of view = 192×192 mm, interleaved slice ordering] and corrected online for head motion. The first 2 volumes were discarded to allow for T1 equilibration effects. Visual stimuli were presented using E-Prime and viewed through a mirror attached to the head coil. In addition to functional imaging, a high resolution T1 scan was acquired for anatomic normalization. Preprocessing of the anatomical and functional data were performed using fMRIPrep1.4rc1 (Esteban et al. 2019).

Anatomical Data Preprocessing

The T1-weighted (T1w) image was skull-stripped and corrected for intensity nonuniformity using ANTs v.2.2.0 (Avants et al. 2008). Brain tissue segmentation of cerebrospinal fluid (CSF), white-matter (WM), and gray-matter (GM) was performed on the brain-extracted T1w using FAST in FSL v.5.0.9 (Zhang et al. 2001). Brain surfaces were reconstructed using FreeSurfer v.6.0.1 (Dale et al. 1999), and the brain mask estimated previously was refined with a custom variation of Mindboggle (Klein et al. 2017). Volume-based spatial normalization to one standard space (MNI152NLin2009cAsym; Fonov et al. 2009) was performed through nonlinear registration with ANTs, using brain-extracted versions of both T1w reference and the T1w template.

Functional Data Preprocessing

For each BOLD run per subject, first a reference volume and its skull-stripped version were generated using a custom methodology of fMRIPrep. The BOLD reference was then coregistered to the T1w reference FreeSurfer, which implements boundarybased registration (Greve and Fischl 2009). Coregistration was configured with 9 degrees of freedom to account for distortions remaining in the BOLD reference. Head-motion parameters with respect to the BOLD reference (transformation matrices, and 6 corresponding rotation and translation parameters) are estimated before any spatiotemporal filtering using FSL (Jenkinson et al. 2002). BOLD runs were slice-time corrected using AFNI (Cox and Hyde 1997). The BOLD time-series were then resampled into MNI space using ANTs. FD and 3 region-wise global signals extracted from CSF, the WM, and the whole-brain masks, respectively, were also computed as confound regressors (Satterthwaite et al. 2013; Power et al. 2014).

Functional Network Construction and Preprocessing

Functional brain networks were constructed and analyzed using the Functional Connectivity (CONN) toolbox in MATLAB (Whitfield-Gabrieli and Nieto-Castanon 2012). Our primary goal was to compare functional connectivity of frontoparietal subnetworks during divergent thinking. We therefore used the 17 networks parcellation of Yeo et al. (2011), which includes the 2 subnetworks of interest (see Dixon et al. 2018): FPCNa and FPCNb. The DN core (DN_core) was included to assess its functional connectivity with the 2 FPCN subnetworks. To replicate and extend this analysis, we used the Schaefer parcellation (Schaefer et al. 2018). The Schaefer atlas was based on the original Yeo parcellation and it provides a finer resolution of anatomical regions within the same large-scale networks. Consistent with Schaefer and other recent work (Murphy et al. 2020), we used the 17 network parcellation with 400 parcels; again, we focused on the 3 networks of interest (FPCNa, FPCNb, and DN_core). Given prior work demonstrating increased coupling between the inferior frontal gyrus (IFG) and DN during creativity tasks (Beaty et al. 2014; Takeuchi et al. 2017), we used a mask of IFG to identify 6 parcels within the FPCNb network that were of additional interest (see Analysis Plan). The finer resolution of the Schaefer atlas permitted a community detection analyses, to examine how the regions within the 3 larger networks cluster together during DT compared to the control condition (OCT) and fixation (baseline). Note that the fixation period was used to obtain a more stable baseline for community detection because it provided more fMRI data to compute communities than the shorter resting-state scan.

Mean BOLD signal (concatenated within-condition) was extracted from the 3 network maps (Yeo et al. 2011) and individual network regions (Schaefer et al. 2018) during the AUT, OCT, and fixation conditions. Bivariate correlations were computed between each pair of networks. We conducted separate second-level analyses for the 3 Yeo networks and Schaefer networks (see Analysis Plan). In a first-level analysis, WM and CSF masks, along with first-order derivatives of motion, were entered as confounds and regressed from the network timeseries. Additional preprocessing steps included high-pass filtering, linear detrending, and regression of outlying functional volumes (FD > 0.5; Power et al. 2012). The onsets and durations of the verbal response periods were regressed to account for expected artifacts related to participant vocalization. We also regressed the onsets and durations of all task events (AUT, OCT, and fixation) to account for potential task-induced responses in the BOLD signal that are unrelated to the cognitive processes of interest (e.g., increased arousal during

For all second-level analyses, t-tests on Fisher's Z-transformed correlations were used to test for differences in functional connectivity between conditions. Correction for multiple comparisons was implemented using false discovery rate (FDR). Seed-to-voxel analyses are reported at a cluster-level threshold of P < 0.05 FDR corrected and a voxelwise threshold of level of P < 0.001 uncorrected; ROI-to-ROI analyses are reported at a ROIlevel when significant at a threshold of P < 0.05 FDR corrected. Connectivity contrasts were conducted using the CONN toolbox, using the following procedures: For ROI-to-ROI level analysis, F-contrasts in ROI-level contrast analyses were implemented as multivariate analyses and evaluated through Wilks lambda statistics. For seed-to-voxel contrast analyses, F-contrasts in voxel-level analyses are implemented as repeated-measures analyses using restricted maximum likelihood estimation of

covariance components and evaluated through F-statistical parameter maps.

Network Topology and Community Detection

We employed 2 complementary approaches to explore the extent to which the DN and FPCNs exhibited differential patterns of functional connectivity during the AUT, OCT, and fixation. First, to visualize network coupling, we used a Kamada-Kawai energy algorithm (Kamada and Kawai 1989) in Pajek software (Mrvar and Batagelj 2016). This algorithm arranges network nodes such that well-connected nodes are pulled closer together in geometric distance whereas weakly connected nodes are placed further apart.

Second, we used a community detection algorithm (Newman and Girvan 2004) to assign nodes to "communities" by comparing the connection density for each node (i.e., the portion of possible edges that are actual connections) against the connection density for each node of a generated null model, such that the internal connection density will maximally exceed the internal density of the null model. Intuitively, this approach places strongly connected nodes within the same community and weakly connected nodes in different communities. Each node is assigned to one community. This process was repeated 5 times, with consensus clustering applied to create a consensus community partition for each participant. Consistent with recommended procedures (Rubinov and Sporns 2011) the community detection algorithm was fit with negative asymmetrical weight, which treats negative correlations as auxiliary to positive correlations, as the latter more directly relate to modular organization (i.e., positive correlations among nodes directly indicate that those nodes correspond to a community, whereas negative correlations can only dissociate nodes from communities).

To quantify the extent to which nodes belonging to one atlasdefined network (e.g., DN nodes) were placed in the same community as other nodes belonging to the same network (e.g., other DN nodes) and different networks (e.g., FPCNa, FPCNb), we first identified-for each participant and each network-which community contained the highest percentage the network's nodes. Higher values in this case indicate that a larger percentage of network nodes were placed within the same community by the detection algorithm. For example, if 53% of a participants' DN nodes were placed in community 1 and the remaining 47% of DN nodes were distributed across the remaining communities, then community 1 would be deemed the "DN-rich" community. Finally, we then calculated "co-assignment" of the other network nodes: the percent of network nodes for each of the other 2 networks that were also placed within this community. Once again, higher values here suggest that the network nodes are more strongly associated with nodes belonging to other networks. We also identified—for each participant individually—which community contained the second highest percentage of DN nodes, and how many nodes from each of the other 2 networks fell within this community as well. This network topology approach is conceptually similar to prior work (Mattar et al. 2015).

Analysis Plan

Our study aimed to test whether frontoparietal subnetworks differentially relate to the DN during creative task performance. First, we sought to replicate the resting-state connectivity profiles of the 2 frontoparietal networks reported in prior

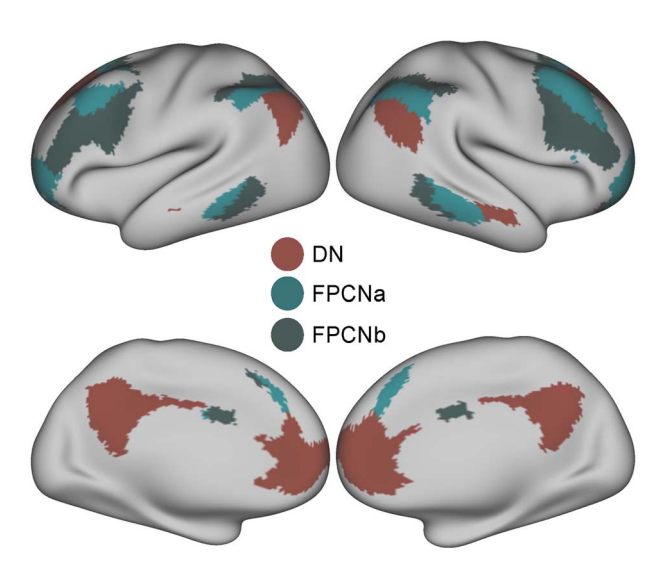


Figure 1. Surface rendering of the default network and frontoparietal subnetworks. Network masks were derived from the Yeo 17-network parcellation and overlaid on an inflated cortical surface using the Connectome Workbench package. DN = default network; FPCNa = frontoparietal control network (subnetwork a); FPCNb = frontoparietal control network (subnetwork b).

work (Dixon et al. 2018). To this end, we conducted ROI-to-ROI and seed-to-voxel functional connectivity analysis on the resting-state data using the 2 frontoparietal subnetworks and the DN from the Yeo 17 networks parcellation as seeds/ROIs. Next, we tested the main question of interest-assessing differential connectivity of frontoparietal subnetworks during divergent creative thinking—by contrasting functional coupling of the networks during the AUT compared to the OCT using both ROI-to-ROI and seed-to-voxel connectivity analyses. To further characterize network relationships associated with divergent thinking, we used a data-driven, community detection approach applied to the Schaefer parcellation to assess how frontoparietal and DN regions cluster together to support divergent thinking. To explore questions related to IFG-DN connectivity specifically, we also assessed the extent to which the FPCNb IFG parcels—compared to the remaining FPCNb parcels and FPCNa-exhibited different patterns of functional connectivity and community assignments with the DN. Finally, we examined individual differences in terms of resting-task correlations and behavioral performance.

Results

Resting-State Connectivity of FPCN Subnetworks

We began by assessing resting-state functional connectivity between FPCN subnetworks to confirm their relationships with the DN reported in recent studies. Figure 1 depicts the 2 FPCNs (FPCNa and FPCNb) and the DN from the Yeo et al. (2011) atlas. We computed 1-sample t-tests (with 0 as a reference) to examine connectivity between networks at rest.

Consistent with prior work, ROI-to-ROI analysis yielded the expected positive correlation between FPCNa and DN: r = 0.06, t(df = 165) = 11.70, P < 0.001. In contrast, we found the expected negative correlation between FPCNb and DN: r = -0.06, t(df = 165) = -11.01, P < 0.001; the 2 frontoparietal networks were positively correlated, as expected: r = 0.14 t(df = 165) =32.48, P < 0.001.

The ROI-to-ROI connectivity pattern above was further confirmed in a series of seed-to-voxel analysis. Using FPCNa as seed, we found significant voxel clusters positively correlated within core default regions: PCC, MPFC, bilateral AG, and bilateral MTG (see Fig. 2). Using FPCNb as seed, we found the opposite profile, with negative connectivity clusters found within the same default regions. Contrasting connectivity associated with FPCNa versus FPCNb yielded a pattern of functional connectivity that mirrored the DN (see Fig. 2). In sum, these results replicate previous findings regarding the relationships between frontoparietal subnetworks and the DN during the resting state (Dixon et al. 2018; Murphy et al. 2020).

Divergent Thinking and FPCN Subnetwork Connectivity

Having confirmed the hypothesized resting-state network relationships, we next examined FPCN subnetwork interactions during the divergent thinking task (AUT) compared to the control task (OCT). We thus contrasted ROI-to-ROI functional connectivity between FPCNa, FPCNb, and DN (3 connections, between all pairs of networks) during the AUT compared to OCT control task. A multivariate general linear model showed a significant effect of condition: F(1, 170) = 7.20, P < 0.05 (FDR corrected). Post-hoc ttests revealed stronger positive functional connectivity between FPCNb and DN during the AUT: t(170) = 2.68, P = 0.008. Thus, the task-based results showed increased coupling between 2 networks (FPCNb and DN) that were negatively correlated at rest.

To explore differences in DN functional connectivity with the IFG and the remainder of the FPCNb—as well as whether connectivity was significantly different for the creative and noncreative task—we conducted 2 (FPCNb parcel: IFG parcels, all remaining non-IFG parcels) × 2 (Task: AUT, OCT) mixed effects ANOVA using the Schaefer atlas parcellation. This model indicated a small, but significant main effect of FPCNb parcel; functional connectivity between the DN and IFG (mean z(r) = 0.05) was greater than that between the DN and the remaining FPCNb parcels (z(r) = 0.04; P = 0.03) across both task conditions. However, this model failed to indicate an effect of task (P=0.09) or an FPCNb parcel \times Task interaction (P = 0.19). Thus, IFG regions of FPCNb were more strongly connected to the DN (relative to remainder of the FPCNb network), with this effect consistent across creative and noncreative task conditions.

Next, we conducted a seed-based analysis to further explore connectivity patterns between the FPCN subnetworks and the rest of the brain during the AUT compared to the OCT control task (see Fig. 3 and Table 1). Compared to FPCNa, FPCNb showed stronger divergent thinking-related functional connectivity with 7 clusters, including 2 regions of the DN core—left angular gyrus (AG) and PCC—as well as the left parahippocampal gyrus (PHG) of the medial temporal lobe subsystem of the DN; additional clusters were found within the frontal and parietal lobes (see Table 1). Compared to FPCNb, FPCNa showed greater divergent thinking-related functional connectivity with 8 clusters, including regions with the DN core: PCC, precuneus, and right AG; additional clusters were found within the parietal and temporal lobes (see Table 1). Thus, both FPCN subnetworks were functionally connected to DN regions and other regions during divergent

To test whether FPCN connectivity related to individual creative ability, we extracted time-series correlations from the ROI-to-ROI analyses for both FPCNs and the DN (FPCNa-DN and FPCNb-DN, separately), for the AUT > OCT contrast, and computed Pearson correlations with semantic distance of AUT

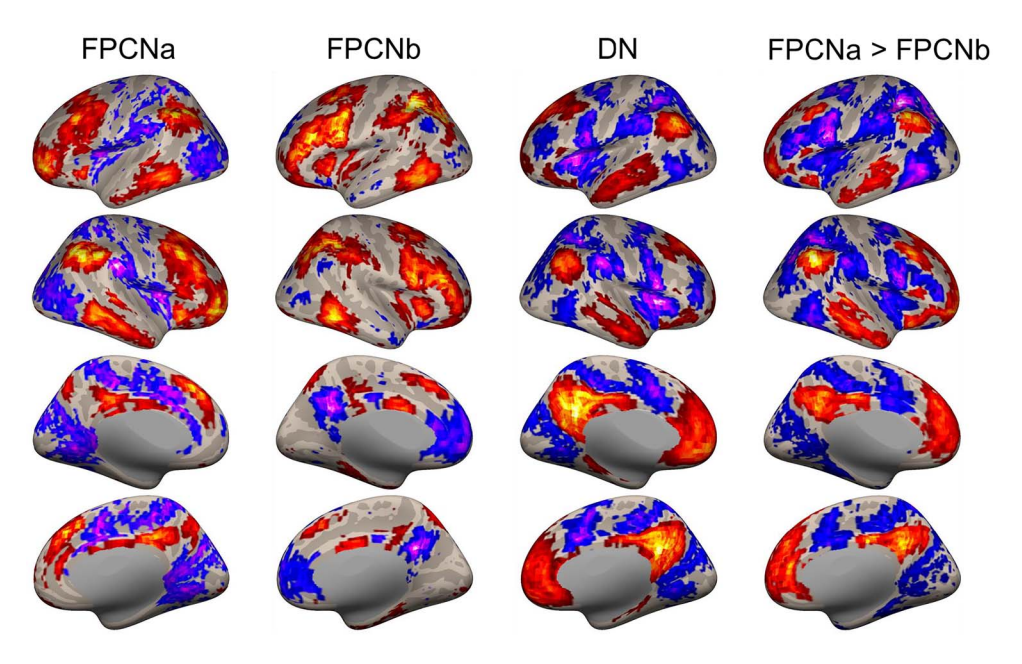


Figure 2. Resting-state seed-to-voxel functional connectivity for two FPCN subnetworks and the DN. Warm colors indicate increased connectivity and cooler colors indicate decreased connectivity. The FPCNa > FPCNb contrast shows similar connectivity as the DN.

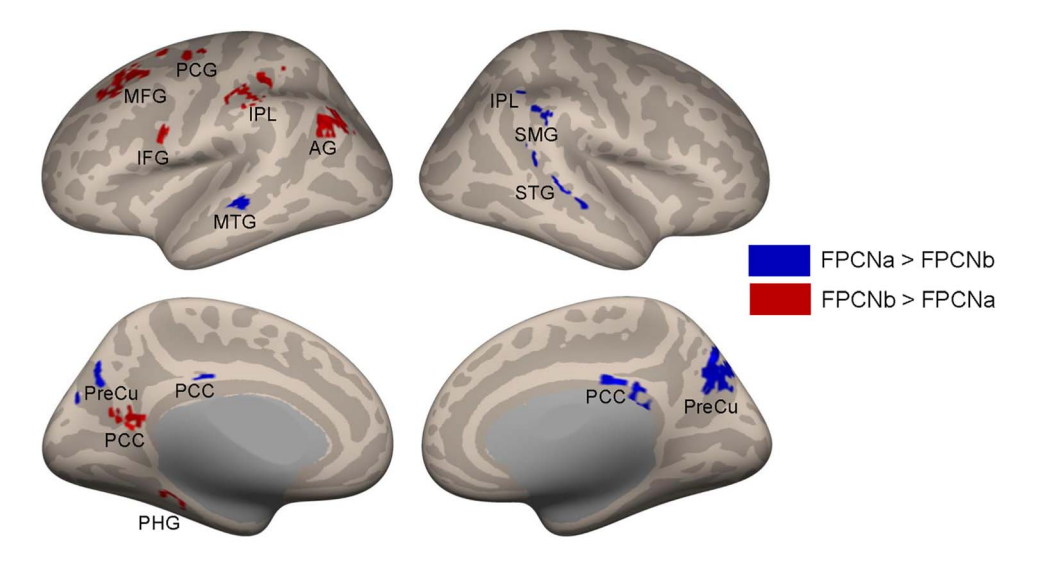


Figure 3. Task-based seed-to-voxel functional connectivity for two FPCN subnetworks during divergent thinking (AUT > OCT). AG=angular gyrus; IFG=inferior frontal gyrus; PCC=posterior cingulate cortex; MFG=middle frontal gyrus; MTG=middle temporal gyrus; PCG=postcentral gyrus; PHG=parahippocampal gyrus; $\label{eq:precure} \textit{PreCu} = \textit{precuneus}; \ \textit{SMG} = \textit{supramarginal gyrus}; \ \textit{STG} = \textit{superior temporal gyrus}.$

responses. We found a modest but statistically significant correlation between FPCNb-DN connectivity strength and semantic distance (r = 0.17, P = 0.03); FPCNa-DN connectivity strength was not significantly related to semantic distance. Next, we examined whether participants with stronger FPCN-DN connectivity (both subnetworks) during the AUT showed stronger coupling at rest. We found a positive correlation between task- and resting-state connectivity for FPCNb-DN (r=0.22, P=0.004); this relationship was not observed for FPCNa-DN connectivity. Participants with stronger FPCNb-DN coupling at rest therefore also showed stronger FPCNb-DN coupling during divergent thinking, suggesting that these participants could more effectively reverse the competitive

resting association between FPCNb and DN to facilitate thinking creatively.

Topological Organization of DN and FPCN

Next, to visualize FPCN and DN topology during the 2 task conditions and fixation, we implemented a Kamada-Kawai energy algorithm. Kamada-Kawai algorithms arrange network nodes such that more strongly connected nodes are placed closer together in geometric distance. This approach allowed us to replicate and extend recent work on FPCN subnetwork topology at rest (fixation) and during cognitive task performance, examining how nodes within the 3 networks cluster together. The

Table 1 Seed-to-voxel functional connectivity analysis for divergent thinking

Seed Region	Peak (MNI)						
	Lat.	ВА	х	у	Z	T _{peak}	k
FPCNa							
MTG	L	21	-52	-31	-7	4.29	336
STG	R	22	47	-29	0	4.66	312
STG	R	13	47	-44	25	4.91	180
PCC	R	23	2	-35	25	5.60	921
PreCu	L	7	-13	-67	32	5.03	530
PreCu	R	7	8	-73	40	5.74	2164
SMG	R	40	56	-46	39	4.24	243
IPL	R	40	41	-52	40	3.96	276
FPCNb							
PHG	L	37	-31	-40	-12	4.66	204
PCC	L	23	-10	-56	8	5.33	540
AG	L	39	-40	-76	35	5.76	1822
IFG	L	9	-55	10	28	5.04	360
IPL	L	40	-58	-29	48	6.28	2149
MFG	L	8	-31	13	53	5.91	2329
MFG	L	6	-28	-8	52	4.23	306

Note: The analysis contrasted AUT > OCT and FPCNa > FPCNb. Lat. = Laterality, BA = Brodmann Area, L/R = Left/Right, k = cluster size, MTG = Middle Temporal Gyrus, $STG = Superior\ Temporal\ Gyrus,\ PCC = Posterior\ Cingulate\ Cortex,\ PreCu = Precuneus,\ SMG = Supramarginal\ gyrus,\ IPL = Inferior\ Parietal\ Lobule,\ PHG = Parahippocampal\ Precuneus,\ PHG = Parahippocampal\ PHG = PARAHI$ Gyrus, AG = Angular gyrus, IFG = Inferior Frontal Gyrus, MFG = Middle Frontal Gyrus

average full sample Z-transformed correlation matrix (FPCNa, FPCNb, and DN nodes within the Schaefer atlas) was thresholded to retain only the top 20% of connections (based on Z values). Visualizations were produced for fixation, AUT, and OCT (Fig. 4).

Kamada-Kawai visualizations indicated stronger withinnetwork FC during fixation and greater between-network FC during the 2 task conditions. That is, network nodes appeared more interconnected during AUT and OCT compared to fixation. In order to quantify these findings, we compared average FC within and between each network during the AUT, OCT, and fixation. Consistent with the visualizations, paired t-tests indicated that FC within each network during fixation was significantly greater than within-network FC during AUT (all t(df = 170) > 7.50, P < 0.0001) and OCT (all t(df = 170) > 7.50, P < 0.0001). Withinnetwork FC was also significantly greater during OCT than AUT for FPCNa (t(df = 170) = 3.86, P = 0.0002) and DN (t(df = 170) = 6.11,P < 0.0001), but not FPCNb (t(df = 170) = 0.70, P = 0.49). Further, all between-network FC was significantly weaker during fixation than during AUT (all t(df = 170) > -7.01, P < 0.0001) and OCT (all t(df = 170) > -5.60, P < 0.0001). Connectivity between the 2 FPCNs was also greater during OCT than during AUT (t(df = 170) = 4.68,P < 0.0001). Together, these findings suggest that the DN and frontoparietal subnetworks exhibit greater decoupling at rest (fixation) than during the AUT or OCT conditions.

Community Detection of DN and FPCN Subnetworks

We next implemented a complimentary approach—community detection—to further quantify differences in FC patterns of the frontoparietal subnetworks and DN at task and during rest. The community detection algorithm (Newman and Girvan 2004) placed nodes into communities such that the internal connection density maximally exceeded the internal density of a null model. That is, strongly connected nodes were more likely to be placed within the same community.

We then examined community coassignment of frontoparietal subnetworks and DN nodes to further evaluate network topology. First, for each network for each participant, we identified which community contained the greatest number of nodes for the corresponding network. We then calculated the percent of each network's nodes that fell within that community, with a larger value indicating that a greater percentage of network nodes were placed in the same community.

Consistent with results using network-to-network FC, a higher percentage of nodes were placed in the same community during fixation than during task for the FPCNb (t(df = 170) > 4.80, P < 0.0001), FPCNa (rest vs. AUT: t(df = 170) = 3.02, P = 0.0029; fixation vs. OCT: t(df = 170) = 1.98, P = 0.049), and DN (t(df = 170) > 9.01, P < 0.0001). That is, nodes that belonged to the same atlasdefined resting-state network exhibited more similar connectivity patterns during fixation than during the 2 task conditions. Thus, these results were consistent with the imposed structure of the brain atlas, since the atlas-defined resting-state networks were more intact (i.e., placed in the same data-driven community more frequently) in the absence of task demands.

To investigate "co-assignment," we calculated the percentage of nodes from the frontoparietal subnetworks that were placed in the DN-rich community (i.e., the community containing the highest percentage of DN nodes). Another series of paired t-tests was performed to examine whether coassignment for both FPCNs was significantly greater during the task conditions than during fixation. Compared with fixation, FPCNb and DN coassignment was significantly greater during both AUT (t(df=170)=10.47, P<0.0001) and OCT (t(df=170)=8.72,P < 0.0001). Coassignment between FPCNa and DN was also higher at task than fixation (AUT: t(df=170)=8.35, P<0.0001; OCT: t(df = 170) = 4.93, P < 0.0001).

We next performed a 2 (FPCN: A, B) × 2 (Task: AUT, OCT) mixed effects ANOVA in order to determine whether

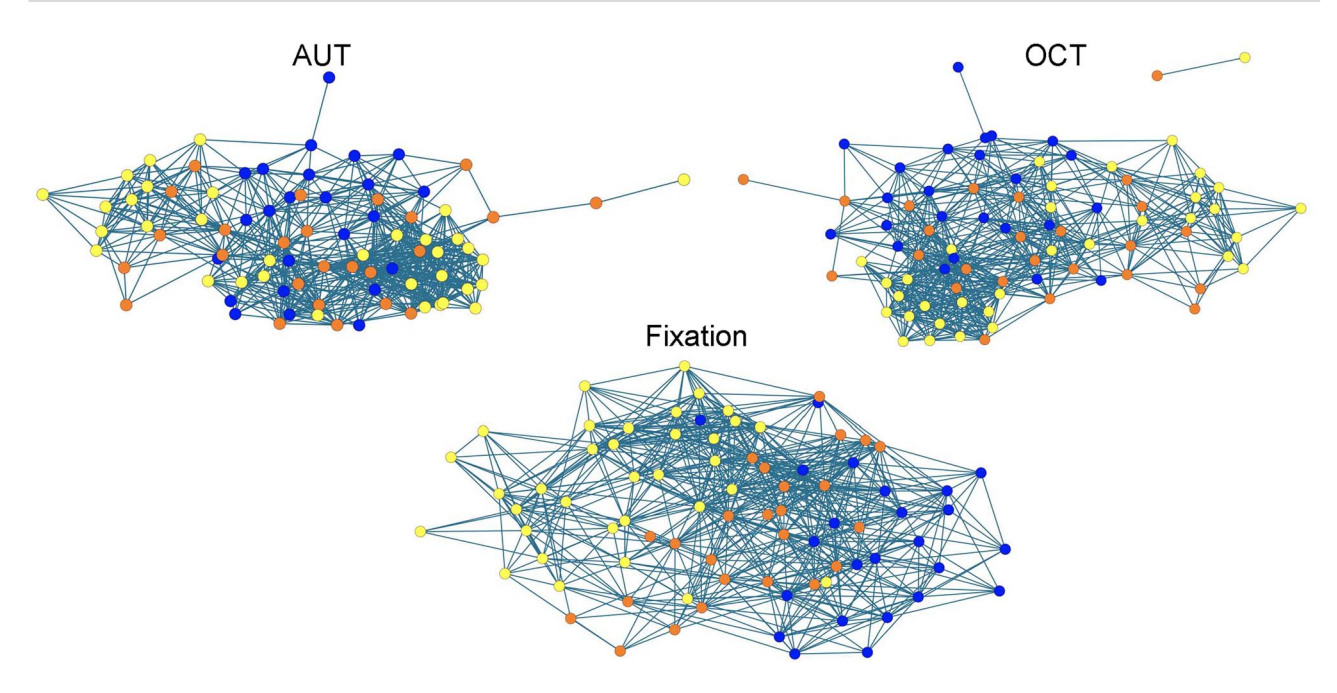


Figure 4. Kamada-Kawai visualizations of network topology during the two task conditions (AUT and OCT) and the baseline condition (Fixation). Orange = FPCNa; Blue = FPCNb; Yellow = DN.

community coassignment of the FPCN nodes to the DN-rich community varied by task condition. This model revealed a significant FPCN \times Task interaction (F(340) = 4.78, P = 0.03), with coassignment greatest for FPCNa and DN during the

Lastly, given prior work indicating particularly strong functional connectivity between the IFG and DN during AUT (Beaty et al. 2014; Takeuchi et al. 2017), we explored the extent to which the increased FPCNb-DN coassignment during the AUT was driven by the IFG. That is, was IFG coassignment to the DN-rich community significantly greater than the coassignment of all the remaining FPCNb parcels to the DN-rich community? Despite greater functional connectivity between the IFG and DN (see Divergent Thinking and FPCN Subnetwork Connectivity), a paired t-test indicated that a larger percentage of the non-IFG regions of FPCNb (23.9%) were placed in the DN-rich community than were the IFG parcels (9.5%, t(170) = 7.38, P < 0.0001). However, when the same question was applied to the community containing the second-most DN nodes (i.e., is there a higher percentage of IFG parcels than non-IFG FPCNb parcels in this community?), results were indeed consistent with functional connectivity analyses as well as prior work; a paired t-test revealed more IFG parcels placed in the same community as the DN (33.4%) than was the remainder of FPCNb (17.8%; t(170) = 7.43, P < 0.0001). Thus, the IFG may play an especially crucial role in DN community organization. That is, the DN may reconfigure into 2 large communities during AUT: one community with the non-IFG regions of FPCNb, and another community with the IFG. Consistent with this interpretation, a 2 (DN community: most DN nodes, second-most DN nodes) × 3 (FPCN: FPCNa, non-IFG FPCNb, IFG) mixed effects ANOVA indicated a significant interaction effect (F(510) = 43.81, P < 0.0001), such that the relative increase in IFG coassignment to the community with the second-most DN nodes was greater than the change for the remainder of FPCN.

Discussion

Creative cognition has been reliably linked to functional connectivity between the frontoparietal (executive) and DNs. Given recent work on frontoparietal subnetwork architecture and functional relationships with the DN—positive DN coupling for one subnetwork (FPCNa) and negative DN coupling for another (FPCNb; Dixon et al. 2018)—we sought to determine whether frontoparietal subnetworks differentially interact with the DN during creative task performance. We conducted a series of functional connectivity analyses (ROI-to-ROI, seed-to-voxel, and community detection), examining both resting-state and task-based connectivity in a large sample. We replicated recent findings regarding resting-state relationships (Dixon et al. 2018; Murphy et al. 2020): FPCNa was positively correlated with the DN and FPCNb was negatively correlated with the DN at rest. The task-based findings, however, revealed a reversal of this functional connectivity pattern during divergent thinking for FPCNb, i.e., positive functional coupling between FPCNb and DN, as well as a greater reorganization of FPCNa regions during the task. At the individual level, we found that more creative people (defined via computational semantic distance) showed stronger functional connectivity between FPCNb (but not FPCNa) and the DN during the divergent thinking task. Collectively, our findings indicate that creative thinking is supported by a functional realignment of a control network that typically shows an antagonistic relationship with the DN, extending recent work on frontoparietal subnetwork interactions and demonstrating their differential dynamics during creative cognition.

Our findings add to the growing literature on the network neuroscience of creative cognition and functional connectivity between FPCN and DN (Ellamil et al. 2012; Jung et al. 2013; Pinho et al. 2016; Beaty et al. 2018, 2019). FPCN-DN interactions have been hypothesized to reflect the top-down regulation of spontaneous cognition, with FPCN guiding and constraining generative processes within the DN (Beaty et al. 2016). In their recent study

of FPCN subnetworks, Dixon et al. (2018) proposed that FPCNa is involved in the regulation of "introspective" cognition. They find that FPCNa functionally connects to the core DN at rest and during several cognitive states, including movie viewing, artwork analysis, evaluation-based introspection, and acceptancebased introspection. In contrast, Dixon et al. found that FPCNb exhibited negative coupling with the core DN at rest and during all task conditions, but positive functional connectivity with the DAN, which supports executive control of attention to external stimuli. A topic-based Neurosynth meta-analysis further found that, although both networks were associated with cognitive control topics (e.g., working memory), FPCNa was associated with introspective topics (e.g., mentalizing, emotion), whereas FPCNb was associated with extrospective topics (e.g., attention, semantics).

A similar pattern of connectivity was reported by Murphy et al. (2020), who examined FPCN activity and connectivity during working memory. Critically, the authors found a dissociation of FPCN subnetwork activity and working memory performance: better working memory was negatively related to FPCNa activity and positively related to FPCNb. Murphy et al. propose a mechanistic framework to describe the competitive relationship between default and control networks, such that the activity of FPCNb governs the connectivity between the larger FPCN and DN. Prior work has found that stronger deactivation of the DN during working memory relates to improved working memory performance, potentially reflecting the suppression of task-irrelevant cognition during an executively demanding task requiring focused attention (Anticevic et al. 2012).

To our knowledge, the current findings are the first to demonstrate a cognitive benefit to increased communication between FPCNb and DN. Although recent work indicates that FPCNa couples with DN to support internally directed cognition (e.g., mentalizing; cf., Dixon et al. 2018), here we showed that both FPCN subnetworks interact with the DN during creative cognition. ROI-to-ROI analyses found stronger functional coupling of FPCNb with DN, yet seed-to-voxel analyses revealed increased connectivity of both FPCNs with DN regions, among other regions. Notably, the positive connectivity pattern observed for FPCNb during the divergent thinking task constitutes a reversal of functional connectivity found for the same individuals during a resting-state scan; the direction of connectivity was comparable for FPCNa at rest and during the task. Individual differences analyses found that more creative individuals—people who produced more semantically distant responses on the AUT—showed stronger connectivity between FPCNb and DN (but not FPCNa and DN). Thus, individual creativity was related to an ability to simultaneously engage networks that work in opposition at rest.

Positive divergent thinking-related functional connectivity between FPNCb and DN-which were negatively correlated at rest—raises questions about the cognitive mechanisms involved. During common executive control tasks (e.g., working memory), the anticorrelation between FPCNb and DN is thought to reflect the suppression of task-unrelated thoughts (i.e., mind wandering) in service of externally focused, goal-directed cognition (Anticevic et al. 2012). Indeed, FPCNb has largely been considered an externally directed network that couples with the DAN (and decouples with the DN) when attention must be focused externally for effective cognitive performance (Spreng et al. 2010; Murphy et al. 2020). However, we show that FPCNb can also cooperate with the DN during a decidedly internally directed cognitive task (i.e., divergent creative thinking).

One possibility is that the unique combination of demands required by creativity tasks, i.e., high demands on internally focused and goal-directed cognition, realigns FPCNb and DN to a "quasi-control" state that may not be otherwise conducive to effective executive control. Although FPCNa has recently been linked to such internally directed, goal-directed cognition (Dixon et al. 2018), we propose that the demands on goal-directed/executive cognition (and therefore FPCNb) are especially high during creative cognition, which requires a range of executive control processes, including working memory updating (Benedek et al. 2014a), controlled semantic retrieval (Silvia et al. 2013), and executive attention (Frith et al. 2021). We thus contend that FPCNb couples with DN to guide, direct, and constrain its activity by inhibiting common ideas, maintaining the task goal, and evaluating candidate ideas for their utility.

Importantly, the community detection analysis provided additional evidence for a role of FPCNa in divergent thinking. Although the community coassignment between both FPCNs and DN was significantly higher during AUT and OCT compared to fixation (i.e., greater task-based realignment compared to rest), the community coassignment of FPCN nodes to the DN-rich community varied by task condition. Specifically, coassignment was greatest for FPCNa and DN during the AUT. Realignment of FPCNa indicates that this control network is more aligned with the DN when people think creatively, consistent with the findings of Dixon et al. (2018) showing a comparable profile for FPCNa during several tasks requiring internally focused cognition. We also identified the IFG as being particularly crucial for DN reconfiguration during AUT; the DN appeared to form 2 large communities—1 with the IFG, and 1 with the rest of FPCN. These findings, based on community coassignment, offer unique insight into the relationship between the FPCN and DN during divergent thinking beyond what can be examined with ROI-to-ROI or seed-to-voxel analyses, which assess connectivity strength between the larger scale networks. Taken together, our findings indicate that both control networks interact with the DN during divergent thinking, but the nature and extent of these interactions differ between networks.

Summary, Limitations, and Future Directions

The present study examined functional connectivity of frontoparietal subnetworks during divergent creative thinking. Despite FPCNb and DN showing an anticorrelated relationship at rest, consistent with recent neuroimaging research (Dixon et al. 2018; Murphy et al. 2020), we found that both FPCNs increased their communication with the DN during the divergent thinking task. A few limitations of the current study should be noted. First, the resting-state fMRI scan occurred after the task-based scan. It is therefore possible that task activation influenced subsequent resting-state connectivity patterns. At the same time, we still observed a reversal in the connectivity patterns of the networks, and one might expect this effect to be even stronger if the resting-state scan occurred before the task-based scan, since any task-related network effect should bias what comes after the scan (but not before). Nevertheless, to address any potential task-based "priming" of resting-state networks, future research should include resting-state scans before and after task scans. Second, the sample was predominantly women (75%), which may limit the generalizability of the findings to a representative sample. Third, our study included a single measure of divergent thinking (i.e., the AUT), which further

constrains the generalizability of our findings to nonverbal

Future research should further investigate the cognitive relevance of frontoparietal subnetworks. FPCNa has been linked to the regulation of introspective cognition (Dixon et al. 2018) whereas FPCNb has been linked to the regulation of extrospective cognition (Murphy et al. 2020). To determine the cognitive roles of FPCN subnetworks in creative cognition, future studies could correlate network activity/connectivity with individual differences in cognitive control abilities that differentially recruit FPCNa and FPCNb, or examine how FPCNs interact with the DN under different task constraints (e.g., inhibiting prepotent associates during idea generation; cf. Beaty et al. 2017a). Nevertheless, given that divergent thinking involves internally directed attention (Benedek 2018), and that FPCNb has been associated with externally directed attention to date (Murphy et al. 2020), our findings suggest that current models of the frontoparietal network should be updated to account for the involvement of both subnetworks in creative cognition. Moreover, in light of the finding that more creative individuals showed stronger divergent thinking-related coupling between networks that were anticorrelated at rest, future research should also examine how the creative brain manages such a functional realignment of networks that typically work in opposition, potentially by tracking the dynamic course of network interactions across time.

Funding

National Science Foundation [DRL-1920653 to A.G. and R.B.]. National Science Foundation [EHR-1661065 to A.G.]. National Science Foundation Graduate Research Fellowship Program [to R.C.]. John Templeton Foundation [ID 61114 to A.W.]. Imagination Institute (www.imagination-institute.org), funded by the John Templeton Foundation [RFP-15-12 to R.B].

Notes

The opinions expressed in this publication are those of the authors and do not necessarily reflect the view of the Imagination Institute or the John Templeton Foundation.

References

- Adnan A, Beaty RE, Lam J, Spreng RN, Turner GR. 2019a. Intrinsic default-executive coupling of the creative aging brain. Soc Cogn Affect Neurosci. 14(3):291-303.
- Adnan A, Beaty RE, Silvia P, Spreng RN, Turner GR. 2019b. Creative aging: functional brain networks associated with divergent thinking in older and younger adults. Neurobiol Aging. 75:150-158.
- Amabile TM. 1983. The social psychology of creativity: a componential conceptualization. J Pers Soc Psychol. 45(2):357-376.
- Andrews-Hanna JR. 2012. The brain's default network and its adaptive role in internal mentation. Neuroscientist. 18(3):251-270.
- Andrews-Hanna JR, Smallwood J, Spreng RN. 2014. The default network and self-generated thought: component processes, dynamic control, and clinical relevance. Ann N Y Acad Sci. 1316(1):29-52.
- Anticevic A, Cole MW, Murray JD, Corlett PR, Wang XJ, Krystal JH. 2012. The role of default network deactivation in cognition and disease. Trends Cogn Sci. 16(12):584-592.

- Avants BB, Epstein CL, Grossman M, Gee JC. 2008. Symmetric diffeomorphic image registration with cross-correlation: evaluating automated labeling of elderly and neurodegenerative brain. Med Image Anal. 12(1):26-41.
- Beaty RE, Silvia PJ. 2012. Why do ideas get more creative across time? An executive interpretation of the serial order effect in divergent thinking tasks. Psychol Aesthet Creat Arts.
- Beaty RE, Benedek M, Wilkins RW, Jauk E, Fink A, Silvia PJ, Hodges DA, Koschutnig K, Neubauer AC. 2014. Creativity and the default network: a functional connectivity analysis of the creative brain at rest. Neuropsychologia. 64:92-98.
- Beaty RE, Benedek M, Kaufman SB, Silvia PJ. 2015. Default and executive network coupling supports creative idea production. Sci Rep. 5:10964.
- Beaty RE, Benedek M, Silvia PJ, Schacter DL. 2016. Creative cognition and brain network dynamics. Trends Cogn Sci. 20(2):
- Beaty RE, Christensen AP, Benedek M, Silvia PJ, Schacter DL. 2017a. Creative constraints: brain activity and network dynamics underlying semantic interference during idea production. Neuroimage. 148:189-196.
- Beaty RE, Silvia PJ, Benedek M. 2017b. Brain networks underlying novel metaphor production. Brain Cogn. 111:163-170.
- Beaty RE, Kenett YN, Christensen AP, Rosenberg MD, Benedek M, Chen Q, Fink A, Qiu J, Kwapil TR, Kane MJ, et al. 2018. Robust prediction of individual creative ability from brain functional connectivity. Proc Natl Acad Sci USA. 115(5): 1087-1092.
- Beaty RE, Seli P, Schacter DL. 2019. Network neuroscience of creative cognition: mapping cognitive mechanisms and individual differences in the creative brain. Curr Opin Behav Sci. 27:22-30.
- Beaty RE, Johnson DR. 2020. Automating creativity assessment with SemDis: an open platform for computing semantic distance. Behav Res Methods. Advance online publication.
- Belden A, Zeng T, Przysinda E, Anteraper SA, Whitfield-Gabrieli S, Loui P. 2020. Improvising at rest: differentiating jazz and classical music training with resting state functional connectivity. Neuroimage. 207:116384.
- Bendetowicz D, Urbanski M, Garcin B, Foulon C, Levy R, Bréchemier ML, Rosso S, de Schotten MT, Volle E. 2018. Two critical brain networks for generation and combination of remote associations. Brain. 141(1):217-233.
- Benedek M, Jauk E, Fink A, Koschutnig K, Reishofer G, Ebner F, Neubauer AC. 2014a. To create or to recall? Neural mechanisms underlying the generation of creative new ideas. Neuroimage. 88:125-133.
- Benedek M, Jauk E, Sommer M, Arendasy M, Neubauer AC. 2014b. Intelligence, creativity, and cognitive control: the common and differential involvement of executive functions in intelligence and creativity. Intelligence. 46:73-83.
- Benedek M, Schües T, Beaty RE, Jauk E, Koschutnig K, Fink A, Neubauer AC. 2018. To create or to recall original ideas: brain processes associated with the imagination of novel object uses. Cortex. 99:93-102.
- Benedek M. 2018. Internally directed attention in creative cognition. In: Jung RE, Vartanian O, editors. The Cambridge handbook of the neuroscience of creativity. Cambridge (UK): Cambridge University Press, pp. 180–194.
- Benedek M, Fink A. 2019. Toward a neurocognitive framework of creative cognition: the role of memory, attention, and cognitive control. Curr Opin Behav Sci. 27:116-122.

- Buckner RL, Andrews-Hanna JR, Schacter DL. 2008. The brain's default network: anatomy, function, and relevance to disease. Ann N Y Acad Sci. 1124(1):1-38.
- Chrysikou EG. 2019. Creativity in and out of (cognitive) control. Curr Opin Behav Sci. 27:94-99.
- Cox RW, Hyde JS. 1997. Software tools for analysis and visualization of fMRI data. NMR Biomed. 10:171-178.
- Dale AM, Fischl B, Sereno MI. 1999. Cortical surface-based analysis: I. segmentation and surface reconstruction. Neuroimage.
- Dixon ML, De La Vega A, Mills C, Andrews-Hanna J, Spreng RN, Cole MW, Christoff K. 2018. Heterogeneity within the frontoparietal control network and its relationship to the default and dorsal attention networks. Proc Natl Acad Sci USA 115(7):E1598-E1607.
- Dumas D, Organisciak P, Doherty P. 2020. Measuring divergent thinking originality with human raters and text-mining models: a psychometric comparison of methods. Psychol Aesthet Creat Arts. Advance online publication.
- Dygert SKC, Jarosz AF. 2020. Individual differences in creative cognition. J Exp Psychol Gen. 149(7):1249-1274.
- Ellamil M, Dobson C, Beeman M, Christoff K. 2012. Evaluative and generative modes of thought during the creative process. Neuroimage. 59(2):1783-1794.
- Esteban O, Markiewicz CJ, Blair RW, Moodie CA, Isik AI, Erramuzpe A, Kent JD, Goncalves M, DuPre E, Snyder M, et al. 2019. fMRIPrep: a robust preprocessing pipeline for functional MRI. Nat Methods. 16:111-116.
- Fink A, Grabner RH, Benedek M, Reishofer G, Hauswirth V, Fally M, Neuper C, Ebner F, Neubauer AC. 2009. The creative brain: investigation of brain activity during creative problem solving by means of EEG and fMRI. Hum Brain Mapp. 30(3):734-748.
- Finke RA, Ward TB, Smith SM. 1992. Creative cognition: theory, research, and applications. Cambridge (MA): MIT Press, p. 256.
- Fonov VS, Evans AC, McKinstry RC, Almli CR, Collins DL. 2009. Unbiased nonlinear average age- appropriate brain templates from birth to adulthood. Neuroimage. 47:S102.
- Fox KCR, Spreng RN, Ellamil M, Andrews-Hanna JR, Christoff K. 2015. The wandering brain: meta- analysis of functional neuroimaging studies of mind-wandering and related spontaneous thought processes. Neuroimage 111(1):611-621.
- Fox MD, Snyder AZ, Vincent JL, Corbetta M, Van Essen DC, Raichle ME. 2005. The human brain is intrinsically organized into dynamic, anticorrelated functional networks. Proc Natl Acad Sci USA. 102(27):9673-9678.
- Frith E, Kane MJ, Welhalf MS, Christensen AP, Silvia PJ, Beaty RE. 2021. Keeping creativity under control: contributions of attention control and fluid intelligence to divergent thinking. Creat Res I.
- Green AE, Cohen MS, Raab HA, Yedibalian CG, Gray JR. 2015. Frontopolar activity and connectivity support dynamic conscious augmentation of creative state. Hum Brain Mapp. 36(3):923-934.
- Green AE. 2016. Creativity, within reason: semantic distance and dynamic state creativity in relational thinking and reasoning. Curr Dir Psychol Sci. 25(1):28-35.
- Greve DN, Fischl B. 2009. Accurate and robust brain image alignment using boundary-based registration. Neuroimage. 48(1):63-72.
- Guilford JP. 1967. The nature of human intelligence. New York (NY): McGraw-Hill, p. 538.
- Jenkinson M, Bannister P, Brady M, Smith S. 2002. Improved optimization for the robust and accurate linear registration

- and motion correction of brain images. Neuroimage. 17(2):
- Jung RE, Mead BS, Carrasco J, Flores RA. 2013. The structure of creative cognition in the human brain. Front Hum Neurosci.
- Jung RE, Chohan MO. 2019. Three individual difference constructs, one converging concept: adaptive problem solving in the human brain. Curr Opin Behav Sci. 27:163-168.
- Kamada T, Kawai S. 1989. An algorithm for drawing general undirected graphs. Inf Process Lett. 31(1):7-15.
- Kaufman JC, Plucker JA, Baer J. 2008. Essentials of creativity assessment. Hoboken (NJ): Wiley, p. 240.
- Kenett YN. 2019. What can quantitative measures of semantic distance tell us about creativity? Curr Opin Behav Sci. 27:11-16.
- Kenett YN, Faust M. 2019. A semantic network cartography of the creative mind. Trends Cogn Sci. 23(4):271-274.
- Klein A, Ghosh SS, Bao FS, Giard J, Häme Y, Stavsky E, Lee N, Rossa B, Reuter M, Neto EC, et al. 2017. Mindboggling morphometry of human brains. PLoS Comput Biol. 13(2):e1005350.
- Liu S, Erkkinen MG, Healey ML, Xu Y, Swett KE, Chow HM, Braun AR. 2015. Brain activity and connectivity during poetry composition: toward a multidimensional model of the creative process. Hum Brain Mapp. 36(9):3351-3372.
- Mandera P, Keuleers E, Brysbaert M. 2017. Explaining human performance in psycholinguistic tasks with models of semantic similarity based on prediction and counting: a review and empirical validation. J Mem Lang. 92:57-78.
- Mattar MG, Cole MW, Thompson-Schill SL, Bassett DS. 2015. A functional cartography of cognitive systems. PLoS Comput Biol. 11(12):e1004533.
- Mednick S. 1962. The associative basis of the creative process. Psychol Rev. 69(3):220-232.
- Mrvar A, Batagelj V. 2016. Analysis and visualization of large networks with program package Pajek. Complex Adapt Syst Model. 4:6.
- Murphy AC, Bertolero MA, Papadopoulos L, Lydon-Staley DM, Bassett DS. 2020. Multimodalnetwork dynamics underpinning working memory. Nat Commun. 11:3035.
- Newman MEJ, Girvan M. 2004. Finding and evaluating community structure in networks. Phys Rev E. 69(2). doi: 026113.
- Niendam TA, Laird AR, Ray KL, Dean YM, Glahn DC, Carter CS. 2012. Meta-analytic evidence for a superordinate cognitive control network subserving diverse executive functions. Cogn Affect Behav Neurosci. 12(2):241-268.
- Orwig W, Diez I, Vannini P, Beaty RE, Sepulcre J. 2021. Creative connections: computational semantic distance captures individual creativity and resting-state functional connectivity. J Cogn Neurosci. 33(3):499-509.
- Pinho AL, Ullén F, Castelo-Branco M, Fransson P, de Manzano Ö. 2016. Addressing a paradox: dual strategies for creative performance in introspective and extrospective networks. Cereb Cortex. 26(7):3052-3063.
- Power JD, Barnes KA, Snyder AZ, Schlaggar BL, Petersen SE. 2012. Spurious but systematic correlations in functional connectivity MRI networks arise from subject motion. Neuroimage. 59(3):2142-2154.
- Power JD, Mitra A, Laumann TO, Snyder AZ, Schlaggar BL, Petersen SE. 2014. Methods to detect, characterize, and remove motion artifact in resting state fMRI. Neuroimage. 84:320-341.
- Prabhakaran R, Green AE, Gray JR. 2014. Thin slices of creativity: using single-word utterances to assess creative cognition. Behav Res Methods. 46(3):641-659.

- Raichle ME, MacLeod AM, Snyder AZ, Powers WJ, Gusnard DA, Shulman GL. 2001. A default mode of brain function. Proc Natl Acad Sci USA. 98(2):676-682.
- Raichle ME. 2015. The brain's default mode network. Annu Rev Neurosci. 38:433-447.
- Rubinov M, Sporns O. 2011. Weight-conserving characterization of complex functional brain networks. Neuroimage.
- Satterthwaite TD, Elliott MA, Gerraty RT, Ruparel K, Loughead J, Calkins ME, Eickhoff SB, Hakonarson H, Gur RC, Gur RE, et al. 2013. An improved framework for confound regression and filtering for control of motion artifact in the preprocessing of resting-state functional connectivity data. Neuroimage. 64:240-256.
- Schaefer A, Kong R, Gordon EM, Laumann TO, Zuo XN, Holmes AJ, Eickhoff SB, Yeo BT. 2018. Local-global parcellation of the human cerebral cortex from intrinsic functional connectivity MRI. Cereb Cortex. 28(9):3095-3114.
- Seeley WW, Menon V, Schatzberg AF, Keller J, Glover GH, Kenna H, Reiss AL, Greicius MD. 2007. Dissociable intrinsic connectivity networks for salience processing and executive control. J Neurosci. 27(9):2349-2356.
- Shi L, Sun J, Xia Y, Ren Z, Chen Q, Wei D, Yang W, Qui J. 2018. Large-scale brain network connectivity underlying creativity in resting-state and task fMRI: cooperation between default network and frontal-parietal network. Biol Psychol. 135:102-111.
- Silvia PJ, Beaty RE, Nusbaum EC. 2013. Verbal fluency and creativity: general and specific contributions of broad retrieval ability (Gr) factors to divergent thinking. Intelligence. 41(5):328-340.
- Spreng RN, Stevens WD, Chamberlain JP, Gilmore AW, Schacter DL. 2010. Default network activity, coupled with the fron-

- toparietal control network, supports goal-directed cognition. Neuroimage. 53(1):303-317.
- Spreng RN. 2012. The fallacy of a "task-negative" network. Front Psychol. 3:145.
- Sunavsky A, Poppenk J. 2020. Neuroimaging predictors of creativity in healthy adults. Neuroimage. 206:116292.
- Takeuchi H, Taki Y, Nouchi R, Yokoyama R, Kotozaki Y, Nakagawa S, Sekiguchi A, Iizueka K, Yamamoto Y, Hanawa S, et al. 2017. Regional homogeneity, resting-state functional connectivity and amplitude of low frequency fluctuation associated with creativity measured by divergent thinking in a sex-specific manner. Neuroimage. 152:258-169.
- Vartanian O, Beatty EL, Smith I, Blackler K, Lam Q, Forbes S. 2018. One-way traffic: the inferior frontal gyrus controls brain activation in the middle temporal gyrus and inferior parietal lobule during divergent thinking. Neuropsychologia. 118:68-78.
- Volle E. 2018. Associative and controlled cognition in divergent thinking: theoretical, experimental, neuroimaging evidence, and new directions. In: Jung RE, Vartanian O, editors. The Cambridge handbook of the neuroscience of creativity. Cambridge (UK): Cambridge University Press, pp. 333-360.
- Whitfield-Gabrieli S, Nieto-Castanon A. 2012. Conn: a functional connectivity toolbox for correlated and anticorrelated brain networks. Brain Connect. 2(3):125-141.
- Yeo BT, Krienen FM, Sepulcre J, Sabuncu MR, Lashkari D, Hollinshead M, Roffman JL, Smoller JW, Zollei L, Polimeni JR, et al. 2011. The organization of the human cerebral cortex estimated by intrinsic functional connectivity. J Neurophysiol. 106(3):1125-1165.
- Zhang Y, Brady M, Smith S. 2001. Segmentation of brain MR images through a hidden markov random field model and the expectation-maximization algorithm. IEEE Trans Med Imaging. 20(1):45-57.